

MAX-phase Ti₂AlC ceramics: syntheses, properties and feasibility of applications in micro electrical discharge machining

Guk-hyun Jeong^a, Gyung-rae Baek^a, Teng Fei Zhang^{b,c}, Kwang Ho Kim^{b,c,d}, Kyujung Kim^e, Hyun Il Shin^f and Myung-Chang Kang^{a,*}

^aGraduate School of Convergence Science, Pusan national University, San 30, Jangjeon-Dong, Geumjeong-Gu, Busan 609-735, Korea

^bNational Core research center for hybrid materials solution (NCRC), Pusan national University, San 30, Jangjeon-Dong, Geumjeong-Gu, Busan 609-735, Korea

^cGlobal Frontier R&D center for Hybrid Interface Materials (GFHIM), Pusan national University, San 30, Jangjeon-Dong, Geumjeong-Gu, Busan 609-735, Korea

^dSchool of Materials Science and Engineering, Pusan national University, San 30, Jangjeon-Dong, Geumjeong-Gu, Busan 609-735, Korea

^eConvergence Research Center of 3D Laser-Aided Innovative Manufacturing Technology, Pusan national University, San 30, Jangjeon-Dong, Geumjeong-Gu, Busan 609-735, Korea

^fSewon R&D Center, Sewon Corporation, 554, Dalseo-Daero, Dalseo-Gu, Daegu 770-130, Korea

MAX-phase Ti₂AlC bulk ceramic was rapidly fabricated by spark plasma sintering (SPS) at 1000 °C and 1100 °C. To obtain monolithic MAX-phase Ti₂AlC, the molar composition (Ti:Al:C) was varied from 1:0.9:1 to 1:1.4:1. The microstructure and material properties of the Ti₂AlC ceramics were systematically investigated. The results show an optimized Al mole fraction of 1.1, with which nearly pure MAX-phase Ti₂AlC ceramics were synthesized. Insufficient or excessive Al content resulted in impurities. The maximum relative density, hardness, electrical and thermal conductivities were also obtained at an Al mole fraction of 1.1. These properties were superior to those of Ti-6Al-4V alloys. The micro-Electrical Discharge Machining (μ-EDM) results showed that the MAX-phase Ti₂AlC ceramics exhibited smaller average micro-hole diameters, shorter machining times, and shorter electrode wear lengths after machining than commercial Ti-6Al-4V alloys, with no obvious local erosion damage near the hole entrance and no tapering effect inside the microholes. This should be attributed to the excellent electrical and thermal characteristics of MAX phases. This demonstrates that MAX-phase Ti₂AlC ceramics are promising candidate for in micro-EDM applications.

Key words: MAX-phase Ti₂AlC, Spark plasma sintering, Mechanical properties, Electrical and thermal conductivities, Oxidation behavior, Micro electrical discharge machining.

Introduction

With recent developments in aerospace, medical, electronics, and automobile industries, there has been a significant increase in the use of high-hardness, ultralight, and difficult-to-cut materials to improve product functionality [1]. In particular, titanium and its alloys possess low density, good ductility, high toughness and stiffness, high corrosion resistance, and good performance at high temperatures, which has made them widely applied as structural materials in engines of automobiles and aircrafts to increase fuel efficiency [2]. However, these materials have high chemical activity, relatively low oxidation resistance and low thermal conductivity. During machining, a large amount of heat will be generated and concentrated on the cutting edges due to low efficient thermal diffusion. Fast oxidation at the

cutting edges will occur, which reduces the toughness and strength of the material, and lead to damages to the cutting edges. Meanwhile, cutting tools are easily worn out due to the heat and their life time will be significantly shorted [3].

Ceramics have many promising properties such as high hardness, high inertness, and high resistance against oxidation and wear, which allows them to be widely used as a structural materials in disk brakes, engine valves of automobiles, and even in the aviation industry [4]. However, most of them are highly brittle with low elasticity, making them difficult to be machined into complex shapes, and in some cases, high-cost special methods such as ultrasonic machining are required for the fabrications [5]. In recent years, a family of distinctive ceramics named M_{n+1}AX_n (abbreviated as MAX, n = 1, 2 or 3) phases have drawn great attention due to their unique properties. The MAX phases are ternary nanolaminates with close-packed hexagonal lattice included in the space group P6₃/mmc, where M is an early transition metal, A is an A-group element,

*Corresponding author:
Tel : +82-51-510-2361
E-mail: kangmc@pusan.ac.kr

and X is nitrogen and/or carbon [6, 7]. Due to the alternating strong covalent M-X and relatively weak metallic M-A bonds, the MAX phases exhibit a unique combination of metallic properties, such as high thermal and electrical conductivities, easy machinability, excellent damage tolerance, and the ceramic properties, such as low density, high Young's modulus, and high resistance against corrosion and oxidation [8-10].

Among MAX-phase materials, the Ti_2AlC is one of the most widely studied member due to its relatively simple component and combination of both advantages of metals and ceramics [11]. Traditional sintering method for MAX-phase Ti_2AlC was reported by Tzenov and Barsoum [12], using the technology of hot isostatic pressing. This method requires a high sintering temperature of 1400 °C, high pressure of 70 MPa, and a long sintering duration of several to dozens of hours. During sintering, some reactants remain unreacted, degrading material properties, and a large amount of energy is needed, giving disadvantage of this method in production efficiency. Recently, many researches have focused on the method of spark plasma sintering (SPS) to synthesize the MAX-phase Ti-Al-C systems [8, 13]. The SPS is a fast sintering process with high energy efficiency, which can fabricate bulk materials with good purity and high density [14]. Meanwhile, due to the relatively low fusing temperature of Al (660 °C), mass loss of Al occurs during sintering MAX-phase Ti_2AlC at high temperatures, which generates impurities like TiC and Al_4C_3 phases [15], making it difficult to synthesize monolithic sintered bodies [16]. Therefore, optimization of raw material ratios of Ti, Al and C powders become more crucial to fabricate MAX-phase Ti_2AlC with high phase purity and density.

Therefore, in this study, MAX-phase Ti_2AlC bulk ceramic was rapidly synthesized at relatively low temperature by SPS from powder mixture of Ti, Al, and TiC, with different mole ratio of Al. The microstructures, electrical and thermal conductivities, mechanical and anti-oxidation properties of the fabricated samples were systematically investigated. On the other hand, except for the chemical and physical properties [17], the machining performance of the MAX phase materials have been rarely reported. While the micro-EDM process is one of the key technologies which is capable of processing microholes and complex forms with high precision, regardless of the material's hardness [18]. Thus, the application potential of the fabricated MAX-phase Ti_2AlC ceramics in micro-EDM process was also evaluated by comparing its microhole diameter and cutting-edge surface with those of the existing commercialized titanium alloy (Ti-6Al-4V) after micro-EDM process.

Experimental Details

Sintering and characterizations of the MAX-phase Ti_2AlC

Ti (99.5%, particle size: 43 μm), Al (99.6%, particle size: 30 μm), and C (99.5%, particle size: 3 μm) powders, purchased from Whole Win (Beijing) Materials Sci. & Tech. Co., Ltd, were used as the raw materials. To obtain monolithic MAX-phase Ti_2AlC , the mole ratio of Ti:Al:TiC was altered from 1 : 0.9 : 1 to 1 : 1.4 : 1. The powders were mixed in a 3D mixer (Korea Material Development Co. Ltd., Korea) at 500 RPM for 12 hrs using stainless balls with diameter of 5 mm. The powders were mixed and collected in a glove filled with Ar gas (99.9%) in order to prevent oxidation. Afterwards, the evenly-mixed powders were inserted into a graphite mold (manufactured by KGT) with a diameter of 30 mm for compressive molding, which was sprayed by boron nitride (BN) to minimize the high-temperature reaction between the graphite mold and the powder.

MAX-phase Ti_2AlC bulk ceramics were synthesized by SPS (SPS-825, SPS Syntex Inc., Japan), with the temperature being raised to 1100 °C at a heating rate of 100 °C/min, under a pressure of 50 MPa for a holding time of 10 min. As seen in Fig. 1, a pulsed DC power with controls on/off ratio of 12 : 2 was applied on the graphite mold. This current generated micro-discharge at the contact points among the particles, and accelerated the thermal effect and electric-field diffusion on the surface of the particles via the heat quantity, which led to rapid sintering. During this process, reaction between Ti and C atoms occurred, with melting Al atoms diffusing and inserting into Ti_2C lattice to form nano-laminated MAX-phase Ti_2AlC .

X-ray diffraction (XRD, D8 ADVANCE, Bruker, Cu $K\alpha$, 40 kV, 40 mA) was used to investigate the phase structure of the Ti_2AlC ceramics. A field emission scanning electron microscope (SEM, F50, FEI, USA) and a transmission electron microscope (TEM, Tecnai G2 F20, FEI, USA) were used to observe the microstructure of the sintered body's fracture plane. To further evaluate the material properties of Ti_2AlC specimens, their hardness and relative density were measured by Vickers indenter (MMT-X, Matsuzawa,

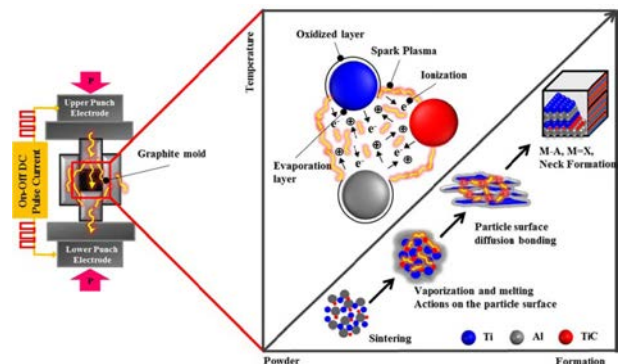


Fig. 1. Basic formation mechanism of the nano-laminated MAX-phase Ti_2AlN by spark plasma sintering.

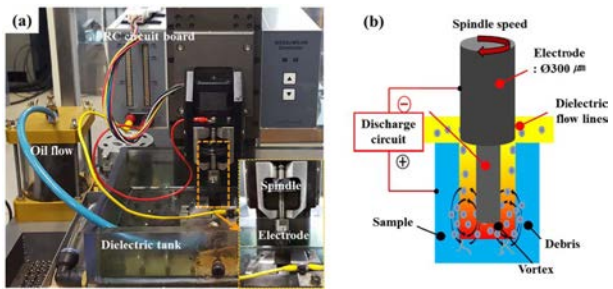


Fig. 2. (a) Experimental device and (b) schematic diagram of the micro-EDM.

Japan) and density tester (XS204, Mettler Toledo, Korea) using Archimedes's method, respectively. The electrical conductivity and thermal conductivity were obtained by measuring the resistivity and thermal diffusion coefficient by a 4-point probe tester (CMT-SR1000N, Advanced Instrument Technology, USA) and a laser flash technique (LFA-457, Netzsch, Germany), respectively. Five measurements were made on each specimens, and the average values and standard deviation were obtained from the measured results. Oxidation tests were performed at 1000 °C in air to observe the oxidation behavior of the MAX-phase Ti_2AlC using a muffle furnace (Up351E, Ajeon Heating Industrial Co., Ltd., Korea) [19, 20].

Micro-EDM behavior of the MAX-phase Ti_2AlC

The micro-EDM equipment (Hyper-15, Hybrid Precision, Korea) is shown in Fig. 2, which is used to assess the machinability of the MAX-phase Ti_2AlC ceramics. RC-type power supply which facilitated the generation of micropulses was attached. The table's scale of movement was 130 mm (x-axis) \times 75 mm (y-axis) \times 80 mm (z-axis), with a resolution of 0.1 μ m in the x- and y-directions. A tungsten round bar with a diameter of 300 μ m was used as the electrode in the micro-EDM process. In addition, an EDM oil of Electro-A class (IME-MH, Oelheld, Germany) was utilized to achieve a smooth electric discharge process. As a comparison, the micro-EDM performance of Ti-6Al-4V alloy, which was commonly applied in high-temperature components, was also investigated by observing the microholes. The thickness of the samples was fixed at 1.5 mm and the electrode's polarity was set to be negative. An optical microscope (KH-8700, Hirox, Japan) and a FE-SEM was used to observe the microholes in the MAX-phase Ti_2AlC and the Ti-6Al-4V alloys after machining.

Results and Discussion

Phase structure of the MAX-phase Ti_2AlC

Fig. 3 presents the XRD patterns of the specimens synthesized at 1100 °C to examine the phase structure change of the Ti_2AlC ceramics as a function of the Al

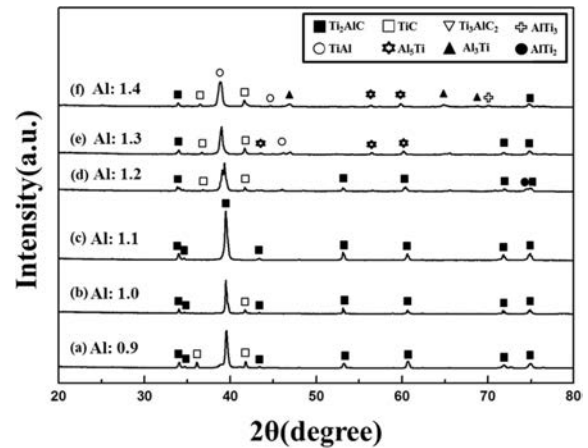


Fig. 3. XRD patterns of the sample synthesized via SPS at 1,100 °C as a function of Al mole fractions: (a) Al: 0.9, (b) Al: 1.0, (c) Al: 1.1, (d) Al: 1.2, (e) Al: 1.3, and (f) Al: 1.4.

mole fraction from 0.9 to 1.4. The sample with an Al mole fraction of 0.9 was mainly composed of MAX-phase Ti_2AlC , while TiC impurity peaks were observed due to the insufficient Al atoms. As the Al mole fraction increased to 1.0, even though the TiC peak was still detected, the diffraction intensity of the TiC peak obviously decreased [21, 22]. It was considered that at the stoichiometric molar ratio of $Ti:Al:TiC = 1:1:1$ for MAX-phase Ti_2AlC , mass loss of the Al occurred during sintering, due to Al evaporation at high temperatures, which led to a non-stoichiometric compound and the formation of the TiC impurity phase [16]. Fully MAX-phase Ti_2AlC ceramic was obtained at the Al mole fraction of 1.1, which demonstrated that slightly excess of Al atoms was necessary to synthesize pure MAX-phase Ti_2AlC . Further increase of Al mole fraction led to impurity phases appeared again. As Al mole fraction increased from 1.2 to 1.4, more and more impurity peaks such as TiC, TiAl, Al_3Ti , and Al_5Ti , etc., were detected with decreased diffraction peak intensity of the Ti_2AlC phase. It was considered that the Al content had exceeded the solubility limit for fabrication of the monolithic MAX-phase Ti_2AlC , resulting in the formation of various Ti-Al alloy phases. It was reported by Hendaoui et al. that in Ti-Al-C systems when the excessive Al mole content exceeds 0.5 mol, the yield of the MAX phase decreases, leading to growth of the $TiAl_3$ phase and a small amount of TiC phase [23]. Hence, in this study, the most appropriate mole ratio of Ti, Al, and C for the synthesis of monolithic MAX-phase Ti_2AlC ceramic was $Ti:Al:C = 1:1.1:1$.

Microstructure of the MAX-phase Ti_2AlC

Fig. 4(a-c) show the SEM cross-sectional images of the Ti_2AlC ceramics with Al mole fraction of 0.9, 1.1 and 1.4, respectively. The phase of the grains was confirmed by EDS analysis. As can be seen, fully

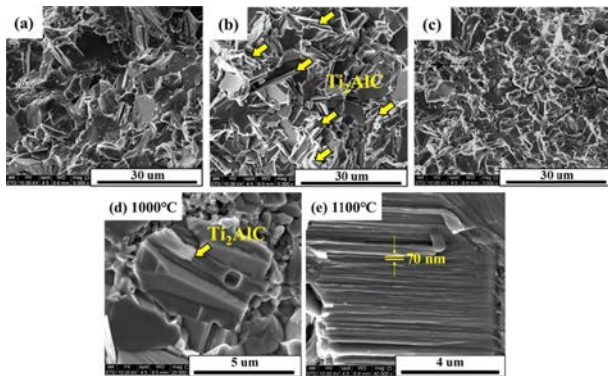


Fig. 4. Cross-sectional SEM images of the Ti₂AlC ceramic synthesized at 1,100 °C with various Al mole fractions: (a) Al: 0.9, (b) Al: 1.1, and (c) Al: 1.4. Cross-sectional SEM images of the Ti₂AlC ceramic with Al mole fraction of 1.1 synthesized at (d) 1000 °C and (e) 1100 °C.

dense bulk ceramics were synthesized by SPS with all Al mole fractions. With Al mole fraction of 0.9 (Fig. 4(a)), only few flake-like grains were observed, which is typical nano-laminated structure of MAX phases [24], and remained un-reacted TiC particles were also observed. While as Al mole fraction increased to 1.1 (Fig. 4(b)), a large number of Ti₂AlC grains with laminated structure were found, demonstrating moderate Al content for the formation of stoichiometric MAX-phase Ti₂AlC ceramics. As Al mole fraction further increased to 1.4 (Fig. 4(c)), the MAX-phase Ti₂AlC grains in the form of laminated structure were not observed and impurity phases appeared. These results showed that the addition of an appropriate mole fraction of Al could produce a monolithic Ti₂AlC ceramic, but an excessive amount resulted in formation of impurities [25]. It also agreed well with the X-ray diffraction patterns shown in Fig. 3.

To investigate the growth process of laminated structure of the MAX-phase Ti₂AlC, higher resolution SEM observation were conducted. Fig. 4(d) shows the SEM image of the fracture plane of the Ti₂AlC ceramic sintered at 1000 °C, where TiC particles were found near the Ti₂AlC grain, as well as the TiAl phases. While at sintering temperature of 1100 °C (Fig. 4(e)), fully laminated structure could be observed, which was the most distinctive characteristic of the MAX-phase Ti₂AlC [26]. According to previous results by Hashimoto et al., in the Ti-Al-C reaction system, the Al fuses at about 660 °C, while at above 900 °C, the fused Al diffuses out and coat the surface of the Ti grains, forming intermetallic TiAl compounds. As the sintering temperature further increases, the TiC phases are spread across the surface of the intermetallic TiAl compounds at a higher rate to form MAX-phase Ti₂AlC with a nanolaminated structure. The detail reactions are shown as follows [27, 28].

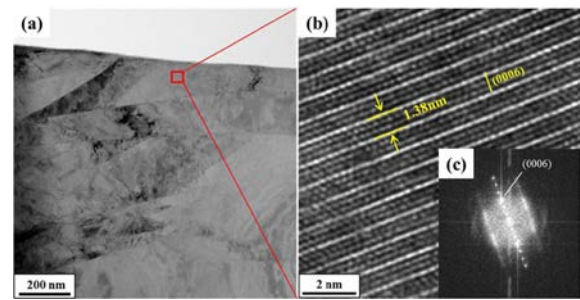
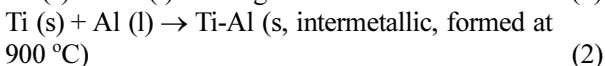


Fig. 5. (a) Bright-field TEM image, (b) HR-TEM image of the MAX-phase Ti₂AlC ceramic synthesized with Al mole fraction of 1.1, and (c) the corresponding selected area diffraction pattern (SADP, insert).

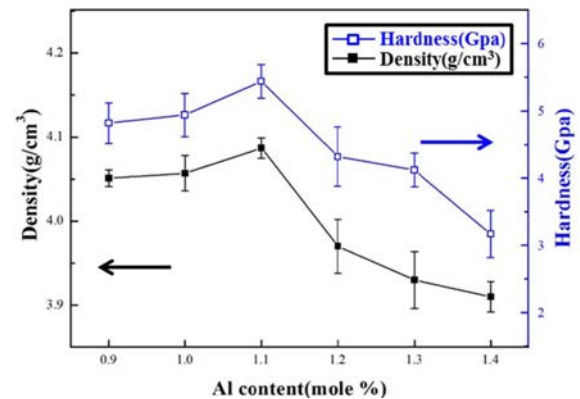


Fig. 6. Variations of relative density and hardness of the Ti₂AlC ceramics as a function of Al mole fraction from 0.9 to 1.4.



To further investigate the microstructure of the MAX-phase Ti₂AlC fabricated at 1000 °C with an Al mole fraction of 1.1, TEM analysis was performed. Fig. 5(a) shows the bright field (BF) TEM image of the Ti₂AlC ceramic, where densely packed grains were observed. While Fig. 5(b) shows the HR-TEM image of the Ti₂AlC ceramic with the corresponding selected area diffraction pattern (SADP) inserted (Fig. 5(c)). From the observations of lattice fringe and the corresponding SADP patterns, the obtained sample was revealed to have well-crystallized MAX-phase Ti₂AlC. The d values of the (0006) planes were perfectly matched with those of the reported MAX-phase Ti₂AlC [29, 30]. MAX-phase Ti₂AlC possessed a hexagonal structure in which covalent Ti₂C layers are intercalated with metallic Al layer.

Density and hardness of the MAX-phase Ti₂AlC

Fig. 6 shows the relative density and hardness of the Ti₂AlC ceramics as a function of the Al mole fraction. The theoretical density of the MAX-phase Ti₂AlC is about 4.11 g/cm³, and its hardness has been reported to be about 2-8 GPa [11]. The relative density and hardness of the Ti₂AlC ceramic synthesized with Al mole fraction of 0.9 were 4.7 GPa and 4.06 g/cm³, respectively. Both

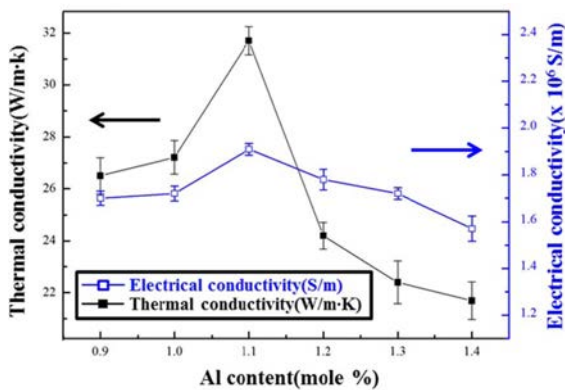


Fig. 7. Variations of thermal and electrical conductivities of the Ti_2AlC ceramic as a function of Al mole fraction from 0.9 to 1.4.

values increased as Al content increased, and the maximum hardness value of 5.4 GPa and relative density of 4.09 g/cm³, which was approaching the theoretical density of the MAX-phase Ti_2AlC , were obtained with an Al mole fraction of 1.1, respectively. However, further increase of the Al mole fraction till 1.2 lead to decline of both the hardness and relative density, which was considered to be attributed to the impurity phases [21, 31, 32], as mentioned in formal sections.

Electrical and thermal conductivities of the MAX-phase Ti_2AlC

Electrical and thermal conductivities of the materials are the key effect factors on Micro-EDM machining process. Fig. 7 shows the electrical and thermal conductivities of the Ti_2AlC ceramics as a function of the Al mole fraction. The thermal conductivity and electrical conductivity of the Ti_2AlC ceramic synthesized with Al mole fraction of 0.9 were 26.2 W/m·K and 1.71×10^6 S/m, respectively. For an Al mole fraction of 1.0, they were 27.1 W/m·K and 1.73×10^6 S/m, respectively. Both thermal conductivity and electrical conductivity increased as Al content increased, and the maximum values of 31.4 W/m·K and 1.91×10^6 S/m were obtained with an Al mole fraction of 1.1, respectively. However, decline of both thermal and electrical conductivities occurred as the Al mole fraction further increased till 1.2. Most of MAX-phase ceramics with nano-laminated structure, such as Ti_3SiC_2 , Ti_3AlC_2 , and Ti_4AlN_3 , have fairly high electrical and thermal conductivities [33]. It was reported that pure MAX-phase Ti_2AlC possess high electrical conductivity of 2.8×10^6 S/m and high thermal conductivity of 46 W/m·K [34], respectively, which are much higher than those of the impure phases such as TiC [35] and TiAl [36]. As mentioned above, moderate Al mole fraction of 1.1 facilitated the synthesis of high-purity MAX-phase Ti_2AlC , which eliminated the impure phases and thereby led to the increase of thermal and electrical conductivities.

Feasibility of the Micro-EDM process for the

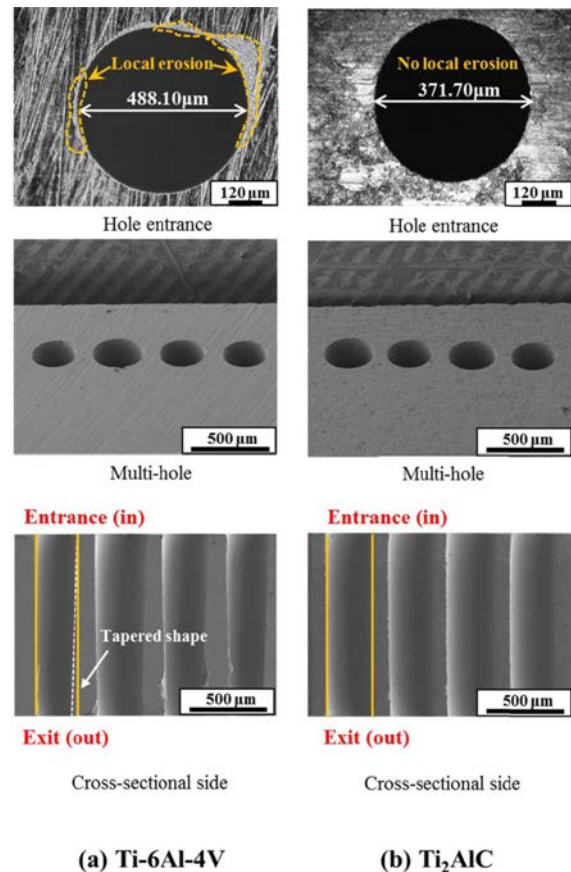


Fig. 8. Evaluation of cutting edges of microholes, diameters of multi-holes, and fractured surface morphology of the (a) Ti-6Al-4V and (b) Ti_2AlC .

MAX-phase Ti_2AlC

Micro-EDM was performed to process microholes in the Ti-6Al-4V alloy and MAX-phase Ti_2AlC ceramic samples, and entrances and cross-sectional images of the microholes are shown in Fig. 8. It can be seen in Fig. 8(a) that local erosion occurred near the hole entrance of the Ti-6Al-4V alloy. Due to relatively low thermal and electrical conductivities of the Ti-6Al-4V alloy, the heat caused by discharge energy was not fully transferred to the material but concentrated at the tip of the electrode during the process. Therefore, the processing material was not fully removed by principle of electric discharge process, but also removed by melting and evaporation effects, which led to this erosion damages at the cutting edge. On the other hand, small debris was produced in the microholes during Micro-EDM process. The debris was discharged out of the microholes from the hole entrance by the flushing effect of the insulating liquid, and the flushing pressure difference increased drastically at the hole entrance [37]. Thus, the debris containing residual thermal energy was also another possible reason for the local erosion damages near the hole entrance of the Ti-6Al-4V alloy.

In contrast, the Ti_2AlC ceramic has better thermal

and electrical conductivities compared with those of the Ti-6Al-4V alloys. It also simultaneously possesses the characteristics of both metals and ceramics, including melting and evaporating properties of the material's, as well as thermal spalling under material removal mechanism. These properties are likely to reduce the effect of pressure difference when large debris is being discharged. As can be seen in Fig. 8(b), no obvious local erosion damage has been observed near the hole entrances. In addition, the microholes processed in the Ti₂AlC ceramic have a diameter of 371.70 μm, whereas those in the Ti-6Al-4V alloy have a much larger diameter of 488.10 μm. The Ti₂AlC ceramic received a large amount of discharge energy, so debris in the form of large thin plates were generally not produced. But smaller debris was generated and discharged from the Ti-6Al-4V alloy, which may result in additional discharge [38]. Short-circuiting may occur and the servo control of the micro-EDM machine will repeat forward and backward movements of the electrode inside the holes. This complex movement will probably led to the abnormally large size of the holes, despite the tungsten electrode's diameter of 300 μm.

To further evaluate the micro-EDM performance, the total machining time and average hole diameter were measured for four processed microholes in the MAX-phase Ti₂AlC ceramic and Ti-6Al-4V alloy. The average hole diameter of the Ti₂AlC ceramic was 380.30 μm, which was much smaller than that of Ti-6Al-4V alloy (409.15 μm). Meanwhile, the machining time of the Ti₂AlC ceramic (137' 57") is 1.7 times shorter than that of the Ti-6Al-4V alloy (237' 18"), and the wear lengths of electrode after machining the Ti₂AlC ceramic (563.00 μm) is 1.3 times shorter than that of the Ti-6Al-4V alloy (757.10 μm). The microholes of both specimens were cut off along cross section and observed to evaluate the taper machinability of the multiple processed microholes. The taper effect was easily found in the microholes of Ti-6Al-4V alloy which developed from the entrance to the exit. While no obvious Tapering was observed in microholes of the Ti₂AlC ceramic, which should be attributed to that the discharge energy was efficiently absorbed by the sintered body due to its excellent electrical and thermal characteristics. Therefore, it can be concluded that the MAX-phase Ti₂AlC ceramics are promising candidate for applications in micro-EDM process.

Conclusions

Dense MAX-phase Ti₂AlC ceramics were fabricated using SPS by varying the Al mole fraction of Ti:Al:C from 1:0.9:1 to 1:1.4:1. The microstructure and material properties of the Ti₂AlC were systematically characterized and the feasibility of applications in micro-EDM machining was also evaluated. The following

results were obtained:

1. The Al mole fraction has big influence in formation of MAX-phase Ti₂AlC and moderate Al mole fraction is important for synthesizing high-purity MAX phases. The optimized Al mole fraction in this study is 1.1, where almost pure MAX-phase Ti₂AlC ceramics were obtained. Deficient and excessive Al content resulted in impurities.

2. The maximum relative density of 4.09 g/cm³ and hardness of 5.4 GPa were obtained with Al mole fraction of 1.1, respectively. Deficient and excessive Al content led to decline of both relative density and the hardness, which should be attributed to the impurity phases. Similar results were also obtained in electrical and thermal conductivities: maximum values of 31.4 W/m·K and 1.91×10^6 S/m were obtained with an Al mole fraction of 1.1, respectively, which were superior than those of the Ti-6Al-4V alloy.

3. The micro-EDM results showed that the MAX-phase Ti₂AlC ceramics exhibited smaller average microhole diameter, shorter machining time, and shorter wear lengths of electrode after machining than those of the commercial Ti-6Al-4V alloy. And Unlike the Ti-6Al-4V alloy, no obvious local erosion damages near the hole entrance and no tapering effect inside the microholes were observed. The superior performance should be attributed to the excellent electrical and thermal characteristics of MAX phases.

Therefore, the MAX-phase Ti₂AlC ceramics are promising candidate for applications in micro-EDM process.

Acknowledgments

Gyung Rae Baek * This author equally contributed as first author.

This research was supported by Global Frontier Program through the Global Frontier Hybrid Interface Materials (GFHIM) of the National Research Foundation of Korea (NRF) funded by the Ministry of Science, ICT & Future Planning (2013M3A6B1078874) and This work was supported by the National Research Foundation of Korea (NRF) Grant funded by the Korean Government (MSIP) (No.2015R1A5A7036513).

References

1. G. Chen, C. Ren, X. Qin, and J. Li, Mater. Design 83 (2015) 598-610.
2. X.G. Lu, C.H. Li, L.Y. Chen, A.T. Qiu, and W.Z. Ding, Mater. Chem. Phys. 129[3] (2011) 718-728.
3. G. Spur and J. Schönbeck, CIRP Ann-Manuf. Tech. 42[1] (1993) 253-256.
4. A. Okada, Mat. Sci. Eng. B-Solid 161[1] (2009) 182-187.
5. H. Nakaoku, T. Masuzawa, and M. Fujino, J. Mater. Process. Tech. 187 (2007) 274-278.
6. T. Zhang, H.B. Myoung, D.W. Shin, and K.H. Kim, J. Ceram. Process. Res. 13 (2012) S149-S153.

7. J. Qin, D. He, C. Chen, J. Wang, J. Hu, and B. Yang, *J. Alloy. Compd.* 462[1] (2008) L24-L27.
8. J. Fu, T. Zhang, Q. Xia, S.H. Lim, Z. Wan, T.W. Lee, and K.H. Kim, *J. Nanomater.* (2015) 2015.
9. N.J. Lane, M. Naguib, J. Lu, P. Eklund, L. Hultman, and M.W. Barsoum, *J. Am. Ceram. Soc.* 95[10] (2012) 3352-3354.
10. E. Ezugwu, and Z.M. Wang, *J. Mater. Process.* 68[3] (1997) 262-274.
11. M. Radovic, and M.W. Barsoum, *Am. Ceram. Soc. Bull.* 92[3] (2013) 20-27.
12. G. Liu, K. Chen, H. Zhou, J. Guo, K. Ren, and J.M.F. Ferreira, *Mater. Lett.* 61[3] (2007) 779-784.
13. S.R. Kulkarni, and A.V.D.K.-H. Wu, *J. Alloy. Compd.* 490[1] (2010) 155-159.
14. N.S. Weston, F. Derguti, A. Tudball, and M. Jackson, *J. Mater. Sci.* 50[14] (2015) 4860-4878.
15. S.C. Tjong, and Z.Y. Ma, *Mater. Sci. Eng. : R: Reports* 29[3] (2000) 49-113.
16. S. Li, W. Xiang, h. Zhai, Y. Zhou, C. Li, and Z. Zhang, *Mater. Res. Bull.* 43[8] (2008) 2092-2099.
17. C. Hu, H. Zhang, F. Li, Q. Huang, and Y. Bao, *Int. J. Refract. Met. H.* 36 (2013) 300-312.
18. H.-S. Tak, J.-H. Kim, H.-S. Lim, C.-T. Lee, Y. -K. Jeong, and M.C. Kang, *J. Kor. Pow. Met. Ins.* 17[4] (2010) 319-325.
19. J. Frodelius, J. Lu, J. Jensen, D. Paul, L. Hultman, and P. Eklund, *J. Eur. Ceram. Soc.* 33[2] (2013) 375-382.
20. M. Sonestedt, J. Frodelius, M. Sundberg, L. Hultman, and K. Stiller, *Corros. Sci.* 52[12] (2010) 3955-3961.
21. T. Ai, F. Wang, X. Feng, and M. Ruan, *Ceram. Int.* 40[7] (2014) 9947-9953.
22. B. Liang, M. Wang, X. Li, S. Sun, Q. Zou, Y. Mu, and X. Li, *J. Alloy. Compd.* 501[1] (2010) L1-L3.
23. A. Hendaoui, D. Vrel, A. Amara, P. Langlois, M. Andasmas, and M. Guerioune, *J. Eur. Ceram. Soc.* 30[4] (2010) 1049-1057.
24. S.-S. Hwang, S.W. Park, J.H. Han, K.S. Han, and T.W. Kim, *J. Kor. Ceram. Soc.* (2003) 40[1] 87-92.
25. J. Yang, C. Liao, J. Wang, Y. Jiang, and Y. He, *Ceram. Int.* 40[3] (2014) 4643-4648.
26. Y. Bai, X. He, R. Wang, Y. Sun, C. Zhu, S. Wang, and G. Chen, *J. Eur. Ceram. Soc.* 33[13] (2013) 2435-2445.
27. M. Yoshida, Y. Hoshiyama, J. Ommyoji, and A. Yamaguchi, *Mater. Sci. Eng. B* 173[1] (2010) 126-129.
28. S. Hashimoto, N. Nishina, K. Hirao, Y. Zhou, H. Hyuga, S. Honda, and Y. Iwamoto, *Mater. Res. Bull.* 47[5] (2012) 1164-1168.
29. Z.J. Lin, M.J. Zhuo, Y.C. Zhou, M.S. Li, and J.Y. Wang, *Acta. mater.* 54[4] (2006) 1009-1015.
30. C. Wang, T. Yang, J. Xiao, S. Liu, J. Xue, J. Wang, Q. Huang, Y. Wang, *Acta Materialia*, 98 (2015) 197-205.
31. J. Zhu, Q. Qi, F. Wang, H. Yang, and Y. Li, *Met. Sci. Heat. Treat.* 53[1-2] (2011) 45-48.
32. S.-L. Xiao, J. Tian, L. -J. Xu, Y.-Y. Chen, H. -B. Yu, and J. -C. Han, 19[6] (2009) 1423-1427.
33. M.W. Barsoum, *Prog. Solid St. Chem.* 28[1] (2000) 201-281.
34. M.W. Barsoum, I. Salama, T.El-Raghy, J. Golczewski, H.J. Seifert, F. Aldinger, W.D. Porter, and H. Wang, *Metall. Mater. Trans. A*, 33[9] (2002) 2775-2779.
35. W. Lengauer, S. Binder, K. Aigner, P. Etmayer, A. Guillou, J. Debuigne, and G. Groboth, *J. Alloy. Compd.* 217[1] (1995) 137-147.
36. W.J. Zhang, B.V. Reddy, and S.C. Deevi, *Scripta. Mater.* 45[6] (2001) 645-651.
37. C.C. Kao, J. Tao, and A.J. Shih, *Int. J. Mach. Tool. Manu.* 47[15] (2007) 2273-2281.
38. S. Kumagai, N. Sato, and K. Takeda, *Int. J. Mach. Tool. Manu.* 46[12] (2006) 1536-1546.